ANALYTICAL AND NUMERICAL TREATMENT TO STUDY THE EFFECTS OF HALL CURRENTS WITH VISCOUS DISSIPATION, HEAT ABSORPTION, AND CHEMICAL REACTION ON PERISTALTIC FLOW OF CARREAU NANOFLUID

by

Naibl T. ELDABE[a], Shaimaa F. RAMADAN[b*], and Amera S. AWAD[b]

[a]Department of Mathematics, Faculty of Education, Ain Shams University, Heliopolis, Cairo, Egypt
[b]Department of Mathematics, Faculty of Science (Girls), Al-Azhar University, Nasr-City, Cairo, Egypt

Original scientific paper
https://doi.org/10.2298/TSCI190319309N

The peristaltic flow of Carreau nanofluid with heat and mass transfer through porous medium inside a symmetric horizontal channel with flexible walls is investigated. The Hall currents with viscous dissipation, heat absorption and chemical reaction are considered, the system is stressed by a uniform strong magnetic field. The problem is modulated mathematically by a system of non-linear PDE which describe the motion, heat and nanoparticles phenomenon of the fluid. These equations with subjected boundary conditions are transferred to a dimensionless form and simplified under the assumptions of long wavelength and low Reynolds number, then solved analytically by using perturbation technique for small Weissenberg number. In other word these equations are solved also numerically by using Runge-Kutta-Merson method with Newton iteration in a shooting and matching technique. The effects of the emerging physical parameters of the problem on the velocity, temperature, and nanoparticles phenomena are discussed numerically for both techniques used for solutions and illustrated graphically through a set of figures. It is found that this problem plays a dramatic role in controlling the solutions. A comparison between the obtained solutions from both methods is made.

Key words: *peristaltic, nanoparticles, heat absorption, chemical reaction, Hall currents, Carreau fluid*

Introduction

Nanofluids are moderately new category of fluids which consist of a base fluid with nano-sized particles (1-100 nm) suspended within them. Water, ethylene glycol, and oil are common examples of base fluids, nanoparticles of materials such as metallic oxides, nitride ceramics, carbide ceramics, and metals have been used for the preparation of nanofluids phenomena. Nanofluids have their enormous applications in heat transfer, such as microelectronics, fuel cells, pharmaceutical processes, and hybrid-powered engines, domestic refrigerator, nuclear reactor coolant, grinding, and space technology, *etc.* They explore enhanced thermal conductivity and the convective heat transfer coefficient is counter balanced to the base fluid. Nanofluids have attracted the attention of many researchers for new production of heat transfer

* Corresponding author, e-mail: shaimaafathey2012@azhar.edu.eg

fluids in heat exchangers, in plants and in automotive cooling significations, due to their extensive thermal properties. A large amount of literature is available which deals with the study of nanofluid and its applications. Nadeem *et al.* [1] have discussed mathematical model for the peristaltic flow of nanofluid through eccentric tubes comprising porous medium. Eldabe *et al.* [2] have investigated the peristaltic transport of MHD Carreau nanofluid with heat and mass transfer inside asymmetric channel. Heat and mass transfer of a Casson nanofluid flow over a porous surface with dissipation, radiation, and chemical reaction have been studied by Palaniammal and Saritha [3]. Peristaltic transport of a nanofluid in an inclined tube has been addressed by Prasad *et al*. [4]. Mahbubul *et al.* [5] have investigated the latest developments on the viscosity of nanofluids. Mustafa *et al.* [6] have obtained the analytical and numerical solutions of the influence of wall properties on the peristaltic flow of a nanofluid.

Peristalsis is a mechanism of fluid transport that occurs due to the propagation of sinusoidal waves across the walls of the channel. This phenomenon widely occurs in several industrial and biomedical applications including swallowing of food through esophagus, chyme motion in the gastrointestinal tract, blood circulation in small blood vessels, sanitary fluid transport of corrosive fluids. Due to the non-linear variation of stress *vs.* deformation rate in many applicable fluids, a number of researchers have been considering the studies of non-Newtonian fluids such as Ellahi *et al.* [7] have discussed a theoretical study of Prandtl nanofluid in a rectangular duct through peristaltic transport. The influence of slip, wall properties on the peristaltic transport of a conducting Bingham fluid with heat transfer have been analyzed by Lakshminarayana *et al.* [8]. Non-linear peristaltic pumping of Johnson-Segalman fluid in an asymmetric channel under effect of magnetic field has investigated by Reddy [9]. The heat transfer analysis for peristaltic mechanism in variable viscosity fluid obtained by Hayat *et al.* [10]. Mahmoud and Abu Oda [11] have analyzed the blood flow in uniform planar channel. Numerical simulation for peristalsis of Carreau-Yasuda nanofluid in curved channel with mixed convection and porous space have initiated by Tanveer *et al.* [12].

The effect of applied magnetic field and heat transfer in the peristaltic flows are also analyzed in view of MHD character of blood, MHD power generators, method of hemodialysis, oxygenation, hyperthermia, and of Hall accelerators as well as in flight MHD. Nowar [13] studied the peristaltic flow of nanofluid under the effect of Hall current and porous medium. Kumar *et al.* [14] have examined the Hall effects on peristaltic flow of couple stress fluid in a vertical asymmetric channel. Hall effect on peristaltic flow of third order fluid in a porous medium with heat and mass transfer have studied by Eldabe *et al.* [15]. Hall effects on the peristaltic transport of Williamson fluid through a porous medium with heat and mass transfer have presented by Eldabe *et al.* [16].

The main aim of this study is to investigate the peristaltic motion of Carreau nanofluid through porous medium in a symmetric horizontal channel. The Hall currents with viscous dissipation, heat absorption and chemical reaction are taken into consideration. The system of PDE which describe this phenomenon with subjected boundary conditions are transferred to a dimensionless form and approximated under the assumption of long wavelength and low Reynolds number assumptions. This system is solved analytically by using the perturbation technique for small Weissenberg number $(\mathrm{W} \ll 1)$ to obtain the velocity distribution, but the homotopy perturbation method is applied to obtain the temperature and nanoparticles phenomena distributions. This system is also resolved numerically by using Runge-Kutta-Merson method with Newton iteration in a shooting and matching technique. The effects of the problem parameters on these solutions are described and cleared graphically.

Basic equations

The basic equations that govern the peristaltic flow of Carreau nanofluid through a porous medium in a symmetric horizontal channel under the effects of Hall current with viscous dissipation, heat absorption and chemical reaction are:

The continuity equation:

$$\nabla \mathbf{V} = 0 \tag{1}$$

Momentum equation:

$$\rho_f \left[\frac{\partial \mathbf{V}}{\partial t} + (\mathbf{V}\nabla)\mathbf{V} \right] = -\nabla P + \nabla \boldsymbol{\tau} + \mathbf{J} \times \mathbf{B} - \frac{\nu}{k_1}\mathbf{V} \tag{2}$$

Energy equation:

$$(\rho c_1)_f \left[\frac{\partial \theta}{\partial t} + (\mathbf{V}\nabla)\theta \right] = k_T \nabla^2 \theta + (\rho c_1)_p \left[D_\mathrm{B} \nabla \theta \nabla \varphi + \left(\frac{D_T}{\theta_0} \right) \nabla \theta \nabla \theta \right] +$$

$$+ \phi + \frac{1}{\sigma} \mathbf{J}\mathbf{J} - Q_0 (\theta - \theta_0) \tag{3}$$

Concentration equation:

$$\left[\frac{\partial \varphi}{\partial t} + (\mathbf{V}\nabla)\varphi \right] = D_\mathrm{B} \nabla^2 \varphi + \left(\frac{D_T}{\theta_0} \right) \nabla^2 T - k_2 (\varphi - \varphi_0) \tag{4}$$

where **V** is the velocity vector of the fluid, **J** – the current density vector including the Hall effect, σ – the electric conductivity, **B** – the magnetic flux density, $\boldsymbol{\tau}$ – the stress tensor, θ – the fluid temperature, φ – the nanoparticle phenomena, ρ_f – the density of the fluid, P – the pressure, k_1 – the permeability of the porous medium, ν – the kinematic viscosity, $(\rho c_1)_\mathrm{f}$ – the heat capacity of the fluid, $(\rho c_1)_\mathrm{f}$ – the heat capacity of the nanoparticle material, k_T – the thermal conductivity, D_B – the Brownian diffusion coefficient, D_T – the thermophoretic coeffecient, Q_o – the heat absorption coefficient, k_2 – the chemical reaction parameter, and ϕ – the dissipation function and is given by $\phi = \tau_{ij}(\partial u_i)/(\partial x_i)$.

Constitutive equation of Carreau fluid [2] is given by:

$$\tau_{ij} = \eta_0 \left(1 + \frac{n-1}{2} \Gamma^2 \dot{\gamma}^2 \right) \dot{\gamma}_{ij} \tag{5}$$

$$\dot{\gamma} = \sqrt{\frac{1}{2} \sum_i \sum_j \dot{\gamma}_{ij} \dot{\gamma}_{ij}} = \sqrt{\frac{1}{2} \Pi} \tag{6}$$

where τ_{ij} is the stress tensor components, η_0 – the zero shear-rate viscosity, n – the dimensionless power-low index, Γ – the time constant, and Π – the second invariant strain tensor.

Mathematical formulation

Consider the peristaltic transport of Carreau nanofluid through porous medium in a symmetric horizontal 2-D channel with flexible walls on which are imposed traveling sinusoidal waves of long wavelength. Choose the Cartesian co-ordinates (X, Y), where X

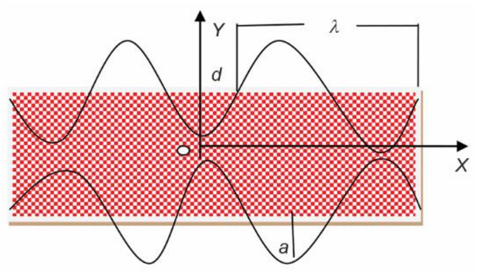

Figure 1. Geometry of the problem

is the axis of the channel and Y – the perpendicular to it. We assume a uniform magnetic field with strong magnetic flux density $\mathbf{B} = (0, 0, B_o)$ and the Hall effects are taken into account. The induced magnetic field is neglected by assuming a very small magnetic Reynolds number, also it is assumed that there is no applied or polarization voltage so that the total electric field $\mathbf{E} = 0$. The lower and upper walls of the channel are maintained at constant temperatures (θ_0 and θ_1), respectively, and concentration (φ_0 and φ_1), respectively. Figure 1 shows the physical mode of a symmetric channel.

The channel wall equation is given by:

$$Y = \pm\eta(X,t) = \pm\left\{d + a\sin\left[\frac{2\pi}{\lambda}(X - ct)\right]\right\} \tag{7}$$

where d is the half width of the channel, a – the amplitude of the wave, λ – the wavelength, t – the time, and c – the wave velocity.

The generalized Ohm's law can be written as:

$$\mathbf{J} = \sigma\left(\mathbf{E} + \mathbf{V}\times\mathbf{B} - \frac{1}{en_\mathrm{e}}\mathbf{J}\times\mathbf{B}\right) \tag{8}$$

where e is the electric charge and n_e – the number density of the electrons. In the view of the above assumption we have:

$$J_x = \frac{\sigma B_0}{1+m^2}(mU + V), \quad J_y = \frac{\sigma B_0}{1+m^2}(mV - U) \tag{9}$$

where U and V are X and Y components of the velocity vector, $m = (\sigma B_0)/(en_\mathrm{e})$ is the Hall parameter.

We introduce a wave frame of reference (x, y) moving with velocity, c, in which the motion becomes independent of time when the channel length is an integral multiple of the wavelength and the pressure difference at the ends of the channel is a constant. The transformation from the fixed frame of reference (X, Y) to the wave frame of reference, (x, y), is given by:

$$x = X - ct, \ \ y = Y, \ \ u = U - c, \ \ v = V, \ \ \text{and} \ \ p(x) = P(X, t) \tag{10}$$

where (u, v) are the velocity components in the wave frame, p and P are pressures in the wave and fixed frames of reference, respectively.

Using the non-dimensional variables:

$$x^* = \frac{x}{\lambda}, \quad y^* = \frac{y}{d}, \quad \eta^* = \frac{\eta}{d}, \quad u^* = \frac{u}{c}, \quad v^* = \frac{v}{c\delta}, \quad \delta = \frac{d}{\lambda}, \quad P^* = \frac{Pd^2}{\eta_0\lambda_c}, \quad \theta^* = \frac{\theta - \theta_0}{\theta_1 - \theta_0},$$

$$\varphi^* = \frac{\varphi - \varphi_0}{\varphi_1 - \varphi_0}, \quad \tau_{ij}{}^* = \frac{\lambda}{c\eta_0}\tau_{ij} \quad i = j, \quad \tau_{ij}{}^* = \frac{d}{c\eta_0}\tau_{ij} \quad i \neq j,$$

$$\dot{\gamma}_{ij}^* = \frac{\lambda}{c\eta_0}\dot{\gamma}_{ij} \quad i = j, \quad \dot{\gamma}_{ij}^* = \frac{d}{c}\dot{\gamma}_{ij} \quad i \neq j \tag{11}$$

Using these information, the governing eqs. of motion (2)-(4) can be written in dimensionless form after dropping the star mark as:

$$\mathrm{Re}\,\delta\left(u\frac{\partial u}{\partial x} + v\frac{\partial u}{\partial y}\right) = -\frac{\partial P}{\partial x} + \delta^2\frac{\partial \tau_{xx}}{\partial x} + \frac{\partial \tau_{xy}}{\partial y} - Au - \frac{M}{1+m^2}(-\delta m v + u + 1) \tag{12}$$

$$\mathrm{Re}\,\delta^3\left(u\frac{\partial v}{\partial x} + v\frac{\partial v}{\partial y}\right) = -\frac{\partial P}{\partial y} + \delta^2\frac{\partial \tau_{xx}}{\partial x} + \delta^2\frac{\partial \tau_{yy}}{\partial y} - \delta^2 A v - \frac{\delta M}{1+m^2}(\delta v + mu + m) \tag{13}$$

$$\mathrm{Re}\,\mathrm{Pr}\,\delta\left(u\frac{\partial \theta}{\partial x} + v\frac{\partial \theta}{\partial y}\right) = \left(\delta^2\frac{\partial^2\theta}{\partial x^2} + \frac{\partial^2\theta}{\partial y^2}\right) + \mathrm{Ec}\,\mathrm{Pr}\left(\delta^2\tau_{xx}\frac{\partial u}{\partial x} + \tau_{xy}\frac{\partial u}{\partial y} + \delta^2\tau_{yy}\frac{\partial v}{\partial y}\right) +$$

$$M\,\mathrm{Ec}\,\mathrm{Pr}[(u+1)^2 + \delta^2 v^2] + N_\mathrm{b}\left(\delta^2\frac{\partial \varphi}{\partial x}\frac{\partial \theta}{\partial x} + \frac{\partial \varphi}{\partial y}\frac{\partial \theta}{\partial y}\right) + N_\mathrm{t}\left[\delta^2\left(\frac{\partial \theta}{\partial x}\right)^2 + \left(\frac{\partial \theta}{\partial y}\right)^2\right] - \gamma\,\mathrm{Pr}\,\theta \tag{14}$$

$$\delta\,\mathrm{Sc}\left(u\frac{\partial \varphi}{\partial x} + v\frac{\partial \varphi}{\partial y}\right) = \left(\delta^2\frac{\partial^2\varphi}{\partial x^2} + \frac{\partial^2\varphi}{\partial y^2}\right) + \frac{N_\mathrm{t}}{N_\mathrm{b}}\left(\delta^2\frac{\partial^2\theta}{\partial x^2} + \frac{\partial^2\theta}{\partial y^2}\right) - S\,\mathrm{Sc}\,\varphi \tag{15}$$

The dimensionless boundary conditions are:

$$\left.\begin{array}{l} u = -1, \quad \theta = 0, \quad \text{and} \quad \varphi = 0, \quad \text{at} \quad y = -\eta \\ u = 1, \quad \theta = 1, \quad \text{and} \quad \varphi = 1, \quad \text{at} \quad y = \eta \end{array}\right\} \tag{16}$$

For long wavelength (*i. e.* $\delta \ll 1$), and low Reynolds number (*i. e.* $\mathrm{Re} \to 0$), the system of our eqs. (13)-(16) can be reduced to:

$$\frac{\partial \tau_{xy}}{\partial y} - Au - \frac{M}{1+m^2}(u+1) = \frac{\partial P}{\partial x} \tag{17}$$

$$\frac{\partial P}{\partial y} = 0 \tag{18}$$

$$\frac{\partial^2\theta}{\partial y^2} + \mathrm{Ec}\,\mathrm{Pr}\,\tau_{xy}\frac{\partial u}{\partial y} + M\,\mathrm{Ec}\,\mathrm{Pr}(u+1)^2 + N_\mathrm{b}\frac{\partial \varphi}{\partial y}\frac{\partial \theta}{\partial y} + N_\mathrm{t}\left(\frac{\partial \theta}{\partial y}\right)^2 - y\,\mathrm{Pr}\,\theta = 0 \tag{19}$$

$$\frac{\partial^2\varphi}{\partial y^2} + \frac{N_\mathrm{t}}{N_\mathrm{b}}\frac{\partial^2\theta}{\partial y^2} - S\,\mathrm{Sc}\,\varphi = 0 \tag{20}$$

From eq. (18), it is clear that P is independent of y. Therefore eqs. (17) and (19) after substituting from eqs. (5) and (6) can be written:

$$\frac{\partial^2 u}{\partial y^2}+3B\mathrm{W}^2\left(\frac{\partial u}{\partial y}\right)^2\frac{\partial^2 u}{\partial y^2}-A_1 u-A_2=0 \tag{21}$$

$$\frac{\partial^2\theta}{\partial y^2}+\mathrm{Ec}\,\mathrm{Pr}\left[\left(\frac{\partial u}{\partial y}\right)^2+B\mathrm{W}^2\left(\frac{\partial u}{\partial y}\right)^4\right]+M\,\mathrm{Ec}\,\mathrm{Pr}(u+1)^2+N_\mathrm{b}\frac{\partial\varphi}{\partial y}\frac{\partial\theta}{\partial y}+N_\mathrm{t}\left(\frac{\partial\theta}{\partial y}\right)^2-\gamma\,\mathrm{Pr}\,\theta=0 \tag{22}$$

where $A_1 = A + M(1 + m^2)$, $A = (\nu d^2)/(\eta_0 k_1)$ is the porosity parameter, $M=(\sigma B_0^2 d^2)/(\eta_0)$ – the magnetic parameter, $A_2 = P_0 + M(1 + m^2)$, $\mathrm{Pr} = (\eta_0 c_1)/k_\mathrm{T}$ – the Prandtl number, $\mathrm{Sc} = (cd)/D_\mathrm{B}$ – the Schmidt number, $\mathrm{Re} = (\rho cd)/\eta_0$ – the Reynolds number, $\mathrm{Ec} = c^2/[c_1(\theta_2 - \theta_1)]$ – the Eckert number, $\gamma = (Q_0 d^2)/k_\mathrm{T}$ – the coefficient of heat absorption, $S = (k_2 d)/c$ – the coefficient of chemical reaction, $N_\mathrm{b} = [(\rho c)_p D_\mathrm{B}(\varphi_1 - \varphi_2)]/[(\rho c)_\mathrm{f}\alpha]$ – the Brownian parameter, $\alpha = k_\mathrm{T}/[(\rho c_1)_\mathrm{f}]$, $N_\mathrm{t} = [(\rho c)_p D_\mathrm{T}(\theta_1 - \theta_0)]/[(\rho c)_\mathrm{f}\alpha T_0]$ – the thermophoresis parameter, $\mathrm{W} = (c\Gamma)/d$ – the Weicsenberg number, $B = (n - 1)/2$, $P_0 = (\mathrm{d}p/\mathrm{d}x)$.

Analytical solution

The momentum eq. (21) subjected to the boundary conditions (16) is solved analytically by using perturbation technique for small Weicsenberg number $(\mathrm{W}\ll 1)$ where:

$$u = u_0 + \mathrm{W}^2 u_1 + O(\mathrm{W}^4) \tag{23}$$

Then the velocity distribution can be written in the form:

$$u(y)=c_1\mathrm{e}^{-y\sqrt{A_1}}+c_2\mathrm{e}^{y\sqrt{A_1}}-\frac{A_2}{A_1}+\mathrm{W}^2\left(\frac{1}{8}\mathrm{e}^{-3y\sqrt{A_1}}\left\{-3BA_1c_1^3-3B\mathrm{e}^{6y\sqrt{A_1}}A_1c_2^3-2\mathrm{e}^{2y\sqrt{A_1}}\cdot\right.\right.$$

$$\left.\left.\cdot[3B(1+2y\sqrt{A_1})A_1c_1^2c_2-4c_3]+2\mathrm{e}^{4y\sqrt{A_1}}[3B(-1+2y\sqrt{A_1})]A_1c_1c_2^2+4c_4\right\}\right) \tag{24}$$

The solutions of energy and mass equations are obtained by applying the homotopy perturbation method, the temperature and the nanoparticles phenomena distributions can be written as:

$$\theta(y)=\frac{y+\eta}{2\eta}+c_5+\frac{1}{192\eta A_1^2}\mathrm{e}^{-4y\sqrt{A_1}}16B\mathrm{e}^{y\sqrt{A_1}}M\mathrm{W}^2\eta A_1(A_1-A_2)c_1^3\,\mathrm{Ec}\,\mathrm{Pr}+$$

$$+3B\mathrm{W}^2\eta A_1^2(3M+5A_1)c_1^4\,\mathrm{Ec}\,\mathrm{Pr}+16B\mathrm{e}^{7y\sqrt{A_1}}M\mathrm{W}^2\eta A_1(A_1-A_2)c_2^3\,\mathrm{Ec}\,\mathrm{Pr}+$$

$$+3B\mathrm{e}^{8y\sqrt{A_1}}\mathrm{W}^2\eta A_1^2(3M+5A_1)c_2^4\,\mathrm{Ec}\,\mathrm{Pr}+96\mathrm{e}^{3y\sqrt{A_1}}M\eta(A_1-A_2)\cdot$$

$$\cdot[c_1(-4+3B\mathrm{W}^2(5+2y\sqrt{A_1})A_1c_1c_2]-4\mathrm{W}^2c_3)\,\mathrm{Ec}\,\mathrm{Pr}+12\mathrm{e}^{2y\sqrt{A_1}}\eta A_1c_1\cdot$$

$$\cdot[-4(M+A_1)c_1+B\mathrm{W}^2A_1(21M+12My\sqrt{A_1}+13A_1+12yA_1^{3/2})c_1^2c_2-8\mathrm{W}^2(M+A_1)c_3]\cdot$$

$$\mathrm{Ec\,Pr} - 96\mathrm{e}^{5y\sqrt{A_1}} M\eta(A_1 - A_2)\{c_2[4 + 3B\mathrm{W}^2(-5 + 2y\sqrt{A_1})A_1c_1c_2] + 4\mathrm{W}^2c_4\}\cdot$$

$$\mathrm{Ec\,Pr} - 12\mathrm{e}^{6y\sqrt{A_1}}\eta A_1c_2(c_2\{4M + A_1[4 + B\mathrm{W}^2(-21M + 12My\sqrt{A_1} - 13A_1 + 12yA_1^{3/2})c_1c_2]\} +$$

$$+ 8\mathrm{W}^2(M + A_1)c_4]\mathrm{Ec\,Pr} + 16\mathrm{e}^{4y\sqrt{A_1}} y(-6\eta A_1^2(yA_3 - 2c_6) + y[\gamma(y + 3\eta)A_1^2 -$$

$$-6\eta(-2MA_1A_2 + MA_2^2 + 3B\mathrm{W}^2A_1^4c_1^2c_2^2 - A_1^3(c_2[c_1(2 + 3BM\mathrm{W}^2c_1c_2) + 2\mathrm{W}^2c_3] +$$

$$+ 2\mathrm{W}^2c_1c_4) + MA_1^2(1 + 2\mathrm{W}^2c_2c_3 + 2c_1(c_2 + \mathrm{W}^2c_4)))h_1)\mathrm{Pr})) + c_9 + yc_{10} +$$

$$+\frac{1}{192\eta^2A_1^2}\left(\frac{4}{5}y^5\gamma^2\eta A_1^2\,\mathrm{Pr}^2 - \frac{3}{16}B\mathrm{e}^{4y\sqrt{A_1}}\mathrm{W}^2\eta A_1(3M + 5A_1)c_2^4\,\mathrm{Ec\,Pr}\,(2\sqrt{A_1}(N_\mathrm{b} + N_\mathrm{t}) - \gamma\eta\,\mathrm{Pr}) +\right.$$

$$+\frac{3}{16}B\mathrm{e}^{-4y\sqrt{A_1}}\mathrm{W}^2\eta A_1(3M + 5A_1)c_1^4\,\mathrm{Ec\,Pr}\,(2\sqrt{A_1}(N_\mathrm{b} + N_\mathrm{t}) + \gamma\eta\,\mathrm{Pr}) +$$

$$+\frac{8}{9}B\mathrm{e}^{3y\sqrt{A_1}}M\mathrm{W}^2\eta(A_1 - A_2)c_2^3\,\mathrm{Ec\,Pr}(-3\sqrt{A_1}(N_\mathrm{b} + N_\mathrm{t}) + 2\gamma\eta\,\mathrm{Pr}) +$$

$$+\frac{8}{9}B\mathrm{e}^{-3y\sqrt{A_1}}M\mathrm{W}^2\eta(A_1 - A_2)c_1^3\,\mathrm{Ec\,Pr}(3\sqrt{A_1}(N_\mathrm{b} + N_\mathrm{t}) + 2\gamma\eta\,\mathrm{Pr}) +$$

$$+\frac{\begin{gathered}48\mathrm{e}^{-y\sqrt{A_1}}M\eta(A_1 - A_2)\,\mathrm{Ec\,Pr}(\sqrt{A_1}(c_1(-4 + 3B\mathrm{W}^2(7 + 2y\sqrt{A_1})A_1c_1c_2) - 4\mathrm{W}^2c_3)(N_\mathrm{b} + N_\mathrm{t}) +\\ + 2\gamma\eta(c_1(-4 + 3B\mathrm{W}^2(9 + 2y\sqrt{A_1})A_1c_1c_2) - 4\mathrm{W}^2c_3)\,\mathrm{Pr})\end{gathered}}{A_1} +$$

$$+\frac{\begin{gathered}48\mathrm{e}^{y\sqrt{A_1}}M\eta(A_1 - A_2)\,\mathrm{Ec\,Pr}(\sqrt{A_1}(c_2(4 + 3B\mathrm{W}^2(-7 + 2y\sqrt{A_1})A_1c_1c_2) + 4\mathrm{W}^2c_4)(N_\mathrm{b} + N_\mathrm{t}) -\\ -2\gamma\eta(c_2(4 + 3B\mathrm{W}^2(-9 + 2y\sqrt{A_1})A_1c_1c_2) + 4W^2c_4)\,\mathrm{Pr})\end{gathered}}{A_1} +$$

$$+48y^2\eta A_1^2(-(c_6 + c_8)N_\mathrm{b} - 2c_6N_\mathrm{t} + 2\gamma\eta c_5\,\mathrm{Pr}) + 3\mathrm{e}^{-2y\sqrt{A_1}}\eta c_1\,\mathrm{Ec\,Pr}(12B\mathrm{W}^2yA_1^3c_1^2c_2(N_\mathrm{b} + N_\mathrm{t}) -$$

$$-4M\sqrt{A_1}(c_1 + 2\mathrm{W}^2c_3)(N_\mathrm{b} + N_\mathrm{t}) + \gamma\eta A_1(c_1(-4 + 33BM\mathrm{W}^2c_1c_2) - 8W^2c_3)\,\mathrm{Pr} -$$

$$-4M\gamma\eta(c_1 + 2\mathrm{W}^2c_3)\,\mathrm{Pr} + B\mathrm{W}^2A_1^2c_1^2c_2(12My(N_\mathrm{b} + N_\mathrm{t}) + 25\gamma\eta\,\mathrm{Pr}) + B\mathrm{W}^2A_1^{5/2}c_1^2c_2\,\cdot$$

$$\cdot(19(N_\mathrm{b} + N_\mathrm{t}) + 12y\gamma\eta\mathrm{P_r}) + A_1^{3/2}((c_1(-4 + 27BM\mathrm{W}^2c_1c_2) - 8\mathrm{W}^2c_3)(N_\mathrm{b} + N_\mathrm{t}) + 12BM\mathrm{W}^2y\gamma\eta c_1^2c_2\,\mathrm{Pr})) +$$

$$+ 6\mathrm{e}^{2y\sqrt{A_1}}\eta c_2\,\mathrm{Ec\,Pr}(6B\mathrm{W}^2yA_1^{3/2}(M + A_1)c_1c_2^2(\sqrt{A_1}(N_\mathrm{b} + N_\mathrm{t}) - \gamma\eta\,\mathrm{Pr}) +$$

$$+\frac{1}{2}(-\sqrt{A_1}(-4(M + A_1)c_2 + B\mathrm{W}^2A_1(27M + 19A_1)c_1c_2^2 - 8\mathrm{W}^2(M + A_1)c_4)(N_\mathrm{b} + N_\mathrm{t}) +$$

$$+\gamma\eta(-4(M+A_1)c_2+B\mathrm{W}^2A_1(33M+25A_1)c_1c_2^2-8\mathrm{W}^2(M+A_1)c_4)\Pr))+$$

$$+8y^3\eta(-4MA_1A_2\,\mathrm{Ec}(N_\mathrm{b}+N_\mathrm{t})\Pr+2MA_2^2\,\mathrm{Ec}(N_\mathrm{b}+N_\mathrm{t})\Pr+6B\mathrm{W}^2A_1^4c_1^2c_2^2\,\mathrm{Ec}(N_\mathrm{b}+N_\mathrm{t})\Pr-$$

$$-2A_1^3(c_2(c_1(2+3BM\mathrm{W}^2c_1c_2)+2\mathrm{W}^2c_3)+2\mathrm{W}^2c_1c_4)\,\mathrm{Ec}(N_\mathrm{b}+N_\mathrm{t})\Pr+$$

$$+A_1^2(4\gamma\eta c_6\Pr+(N_\mathrm{b}+N_\mathrm{t})(2A_3+(-\gamma+2M(1+2c_2(c_1+\mathrm{W}^2c_3)+2\mathrm{W}^2c_1c_4)h_1)\Pr)-SN_\mathrm{b}\,\mathrm{Sc}))-$$

$$-2y^4(-8M\gamma\eta^2A_1A_2\,\mathrm{Ec}\Pr^2+4M\gamma\eta^2A_2^2\,\mathrm{Ec}\Pr^2+12B\mathrm{W}^2\gamma\eta^2A_1^4c_1^2c_2^2\,\mathrm{Ec}\Pr^2-4\gamma\eta^2A_1^3\,\cdot$$

$$\cdot(c_2(c_1(2+3BM\mathrm{W}^2c_1c_2)+2\mathrm{W}^2c_3)+2\mathrm{W}^2c_1c_4)\,\mathrm{Ec}\Pr^2+A_1^2(\gamma\Pr(N_\mathrm{b}+N_\mathrm{t}+2\eta^2\,\cdot$$

$$\cdot(2A_3+(-\gamma+2M(1+2c_2(c_1+\mathrm{W}^2c_3)+2\mathrm{W}^2c_1c_4)h_1)\Pr))+SN_\mathrm{b}\,\mathrm{Sc})))\tag{25}$$

$$\varphi(y)=\frac{y+\eta}{2\eta}+c_7+yc_8-\frac{1}{16\eta A_1^2N_b}\bigg(\frac{4}{3}B\mathrm{e}^{-3y\sqrt{A_1}}M\mathrm{W}^2\eta A_1(A_1-A_2)c_1^3\,\mathrm{Ec}\,N_\mathrm{t}\Pr+$$

$$+\frac{1}{4}B\mathrm{e}^{-4y\sqrt{A_1}}\mathrm{W}^2\eta A_1^2(3M+5A_1)c_1^4\,\mathrm{Ec}\,N_\mathrm{t}\Pr+\frac{4}{3}B\mathrm{e}^{3y\sqrt{A_1}}M\mathrm{W}^2\eta A_1(A_1-A_2)c_2^3\,\mathrm{Ec}\,N_\mathrm{t}\Pr+$$

$$+\frac{1}{4}B\mathrm{e}^{4y\sqrt{A_1}}\mathrm{W}^2\eta A_1^2(3M+5A_1)c_2^4\,\mathrm{Ec}\,N_\mathrm{t}\Pr+8\mathrm{e}^{-y\sqrt{A_1}}M\eta(A_1-A_2)(c_1(-4+3B\mathrm{W}^2\,\cdot$$

$$\cdot(5+2y\sqrt{A_1})A_1c_1c_2)-4\mathrm{W}^2c_3)\,\mathrm{Ec}\,N_\mathrm{t}\Pr+\mathrm{e}^{-2y\sqrt{A_1}}\eta A_1c_1(-4(M+A_1)c_1+$$

$$+\mathrm{W}^2A_1(21M+12My\sqrt{A_1}+13A_1+12yA_1^{3/2})c_1^2c_2-8\mathrm{W}^2(M+A_1)c_3)\,\mathrm{Ec}\,N_\mathrm{t}\Pr-$$

$$-B8\mathrm{e}^{y\sqrt{A_1}}M\eta(A_1-A_2)(4c_2+3B\mathrm{W}^2(-5+2y\sqrt{A_1})A_1c_1c_2^2+4\mathrm{W}^2c_4)\,\mathrm{Ec}\,N_\mathrm{t}\Pr-$$

$$-\mathrm{e}^{2y\sqrt{A_1}}\eta A_1c_2(4(M+A_1)c_2+B\mathrm{W}^2A_1(-21M+12My\sqrt{A_1}-13A_1+12yA_1^{3/2})c_1c_2^2+$$

$$+8W^2(M+A_1)c_4)\,\mathrm{Ec}\,N_\mathrm{t}\Pr+\frac{4}{3}y^3A_1^2(\gamma N_t\Pr-SN_\mathrm{b}\,\mathrm{Sc})-4y^2\eta(-4MA_1A_2\,\mathrm{Ec}\,N_\mathrm{t}\Pr+$$

$$+2MA_2^2\,\mathrm{Ec}\,N_\mathrm{t}\Pr+6B\mathrm{W}^2A_1^4c_1^2c_2^2\,\mathrm{Ec}\,N_\mathrm{t}\Pr-2A_1^3(c_2(c_1(2+3BM\mathrm{W}^2c_1c_2)+2W^2c_3)+$$

$$+2\mathrm{W}^2c_1c_4)\,\mathrm{Ec}\,N_\mathrm{t}\Pr+A_1^2(N_\mathrm{t}(2A_3+(-\gamma+2M(1+2c_2(c_1+\mathrm{W}^2c_3)+2W^2c_1c_4)h_1)\Pr)+SN_\mathrm{b}\,\mathrm{Sc})))+c_{11}+$$

$$+yc_{12}+\frac{1}{192\eta^2A_1^2N_\mathrm{b}}(48y^2\eta A_1^2(N_\mathrm{t}((c_6+c_8)N_\mathrm{b}+2c_6N_\mathrm{t}-2\gamma\eta c_5\Pr)+2S\eta c_7N_\mathrm{b}\,\mathrm{Sc})+$$

$$+\frac{8}{9}B\mathrm{e}^{3y\sqrt{A_1}}M\mathrm{W}^2\eta(A_1-A_2)c_2^3\,\mathrm{Ec}\,N_\mathrm{t}\Pr(3\sqrt{A_1}(N_\mathrm{b}+N_\mathrm{t})-2\eta(\gamma\Pr+S\,\mathrm{Sc}))+$$

$$+\frac{3}{16}Be^{4y\sqrt{A_1}}\mathrm{W}^2\eta A_1(3M+5A_1)c_2^4\,\mathrm{Ec}\,N_\mathrm{t}\,\mathrm{Pr}(2\sqrt{A_1}(N_\mathrm{b}+N_\mathrm{t})-\eta(\gamma\,\mathrm{Pr}+S\,\mathrm{Sc}))-$$

$$-\frac{3}{16}Be^{-4y\sqrt{A_1}}\mathrm{W}^2\eta A_1(3M+5A_1)c_1^4\,\mathrm{Ec}\,N_\mathrm{t}\,\mathrm{Pr}(2\sqrt{A_1}(N_\mathrm{b}+N_\mathrm{t})+\eta(\gamma\,\mathrm{Pr}+S\,\mathrm{Sc}))-$$

$$-\frac{8}{9}Be^{-3y\sqrt{A_1}}M\mathrm{W}^2\eta(A_1-A_2)c_1^3\,\mathrm{Ec}\,N_\mathrm{t}\,\mathrm{Pr}(3\sqrt{A_1}(N_\mathrm{b}+N_\mathrm{t})+2\eta(\gamma\,\mathrm{Pr}+S\,\mathrm{Sc}))-$$

$$-\frac{4}{5}y^5\eta A_1^2(-S^2N_\mathrm{b}\,\mathrm{Sc}^2+\gamma N_\mathrm{t}\,\mathrm{Pr}(\gamma\,\mathrm{Pr}+S\,\mathrm{Sc}))+8y^3\eta(4MA_1A_2\,\mathrm{Ec}\,N_t(N_\mathrm{b}+N_\mathrm{t})\,\mathrm{Pr}-$$

$$-2MA_2^2\,\mathrm{Ec}\,N_\mathrm{t}(N_\mathrm{b}+N_\mathrm{t})\,\mathrm{Pr}-6B\mathrm{W}^2A_1^4c_1^2c_2^2\,\mathrm{Ec}\,N_\mathrm{t}(N_\mathrm{b}+N_\mathrm{t})\,\mathrm{Pr}+2A_1^3(c_2(c_1(2+3BM\mathrm{W}^2c_1c_2)+$$

$$+2\mathrm{W}^2c_3)+2\mathrm{W}^2c_1c_4)\,\mathrm{Ec}\,N_\mathrm{t}(N_\mathrm{b}+N_\mathrm{t})\,\mathrm{Pr}-A_1^2(N_\mathrm{t}(4\gamma\eta c_6\,\mathrm{Pr}+(N_\mathrm{b}+N_\mathrm{t})(2A_3+$$

$$+(-\gamma+2M(1+2c_2(c_1+\mathrm{W}^2c_3)+2\mathrm{W}^2c_1c_4)h_1)\,\mathrm{Pr}))-SN_\mathrm{b}(4\eta c_8+N_\mathrm{t})\,\mathrm{Sc}))-$$

$$-\frac{1}{A_1}48e^{-y\sqrt{A_1}}M\eta(A_1-A_2)\,\mathrm{Ec}\,N_\mathrm{t}\,\mathrm{Pr}(6B\mathrm{W}^2yA_1^2c_1^2c_2(N_\mathrm{b}+N_\mathrm{t})-4\sqrt{A_1}(c_1+\mathrm{W}^2c_3)(N_\mathrm{b}+N_\mathrm{t})+$$

$$+54B\mathrm{W}^2\eta A_1c_1^2c_2(\gamma\,\mathrm{Pr}+S\,\mathrm{Sc})-8\eta(c_1+\mathrm{W}^2c_3)(\gamma\,\mathrm{Pr}+S\,\mathrm{Sc})+3B\mathrm{W}^2A_1^{3/2}c_1^2c_2\,\cdot$$

$$\cdot(7N_\mathrm{b}+7N_\mathrm{t}+4y\eta(\gamma\,\mathrm{Pr}+S\,\mathrm{Sc})))+\frac{1}{A_1}48e^{y\sqrt{A_1}}M\eta(A_1-A_2)\,\mathrm{Ec}\,N_\mathrm{t}\,\mathrm{Pr}\,(-6B\mathrm{W}^2yA_1^2c_1c_2^2(N_\mathrm{b}+N_\mathrm{t})-$$

$$-4\sqrt{A_1}(c_2+\mathrm{W}^2c_4)(N_\mathrm{b}+N_\mathrm{t})-54B\mathrm{W}^2\eta A_1c_1c_2^2(\gamma\,\mathrm{Pr}+S\,\mathrm{Sc})+8\eta(c_2+\mathrm{W}^2c_4)(\gamma\,\mathrm{Pr}+S\,\mathrm{Sc})+$$

$$+3B\mathrm{W}^2A_1^{3/2}c_1c_2^2(7N_\mathrm{b}+7N_\mathrm{t}+4y\eta(\gamma\,\mathrm{Pr}+S\,\mathrm{Sc})))-3e^{-2y\sqrt{A_1}}\eta c_1\,\mathrm{Ec}\,N_\mathrm{t}\,\mathrm{Pr}(12B\mathrm{W}^2yA_1^3c_1^2c_2(N_\mathrm{b}+N_\mathrm{t})-$$

$$-4M\sqrt{A_1}(c_1+2\mathrm{W}^2c_3)(N_\mathrm{b}+N_\mathrm{t})+\eta A_1(c_1(-4+33BM\mathrm{W}^2c_1c_2)-8\mathrm{W}^2c_3)(\gamma\,\mathrm{Pr}+S\,\mathrm{Sc})-$$

$$-4M\eta(c_1+2\mathrm{W}^2c_3)(\gamma\,\mathrm{Pr}+S\,\mathrm{Sc})+B\mathrm{W}^2A_1^2c_1^2c_2(12My(N_\mathrm{b}+N_\mathrm{t})+25\eta(\gamma\,\mathrm{Pr}+S\,\mathrm{Sc}))+$$

$$+B\mathrm{W}^2A_1^{5/2}c_1^2c_2(19N_\mathrm{b}+19N_\mathrm{t}+12y\eta(\gamma\,\mathrm{Pr}+S\,\mathrm{Sc}))+A_1^{3/2}(-4c_1(N_\mathrm{b}+N_\mathrm{t})-8\mathrm{W}^2c_3(N_\mathrm{b}+N_\mathrm{t})+$$

$$+3BM\mathrm{W}^2c_1^2c_2(9N_\mathrm{b}+9N_\mathrm{t}+4y\eta(\gamma\,\mathrm{Pr}+S\,\mathrm{Sc}))))+3e^{2y\sqrt{A_1}}\eta c_2\,\mathrm{Ec}\,N_\mathrm{t}\,\mathrm{Pr}\,\cdot$$

$$\cdot(-12B\mathrm{W}^2yA_1^3c_1c_2^2(N_\mathrm{b}+N_\mathrm{t})-4M\sqrt{A_1}(c_2+2\mathrm{W}^2c_4)(N_\mathrm{b}+N_\mathrm{t})-\eta A_1(c_2(-4+33BM\mathrm{W}^2c_1c_2)-$$

$$-8\mathrm{W}^2c_4)(\gamma\,\mathrm{Pr}+S\,\mathrm{Sc})+4M\eta(c_2+2\mathrm{W}^2c_4)(\gamma\,\mathrm{Pr}+S\,\mathrm{Sc})-B\mathrm{W}^2A_1^2c_1c_2^2(12My(N_\mathrm{b}+N_\mathrm{t})+$$

$$+25\eta(\gamma\,\mathrm{Pr}+S\,\mathrm{Sc}))+B\mathrm{W}^2A_1^{5/2}c_1c_2^2(19N_\mathrm{b}+19N_\mathrm{t}+12y\eta(\gamma\,\mathrm{Pr}+S\,\mathrm{Sc}))+A_1^{3/2}(-4c_2(N_\mathrm{b}+N_\mathrm{t})-$$

$$-8\mathrm{W}^2c_4(N_\mathrm{b}+N_\mathrm{t})+3BM\mathrm{W}^2c_1c_2^2(9N_\mathrm{b}+9N_\mathrm{t}+4y\eta(\gamma\,\mathrm{Pr}+S\,\mathrm{Sc}))))+$$

$$+2y^4(-8M\eta^2A_1A_2\,\mathrm{Ec}\,N_\mathrm{t}\,\mathrm{Pr}(\gamma\,\mathrm{Pr}+S\,\mathrm{Sc})+4M\eta^2A_2^2\,\mathrm{Ec}\,N_\mathrm{t}\,\mathrm{Pr}(\gamma\,\mathrm{Pr}+SS_\mathrm{c})+$$
$$+12B\mathrm{W}^2\eta^2A_1^4c_1^2c_2^2\,\mathrm{Ec}\,N_\mathrm{t}\,\mathrm{Pr}(\gamma\,\mathrm{Pr}+S\mathrm{Sc})-4\eta^2A_1^3(3BM\mathrm{W}^2c_1^2c_2^2+2\mathrm{W}^2c_2c_3+$$
$$+2c_1(c_2+\mathrm{W}^2c_4))\,\mathrm{Ec}\,N_\mathrm{t}\,\mathrm{Pr}(\gamma\,\mathrm{Pr}+S\,\mathrm{Sc})+A_1^2+(4\eta^2A_3N_\mathrm{t}(\gamma\,\mathrm{Pr}+S\,\mathrm{Sc})+N_\mathrm{t}\cdot$$
$$+\mathrm{Pr}(\gamma N_\mathrm{t}-2\eta^2(\gamma-2M(1+2c_2(c_1+\mathrm{W}^2c_3)+2\mathrm{W}^2c_1c_4)h_1)(\gamma\,\mathrm{Pr}+S\,\mathrm{Sc}))+$$
$$+N_\mathrm{b}(2S^2\eta^2\,\mathrm{Sc}^2+N_\mathrm{t}(\gamma\,\mathrm{Pr}+S\,\mathrm{Sc})))))\tag{26}$$

Numerical solution

The same system of our non-liner PDE is solved by the numerical method based on Runge-Kutta-Merson method with Newton iteration in a shooting and matching technique. Use the following transformations:

$$u=Y_1,\qquad \theta=Y_3,\qquad \varphi=Y_5$$

Equations (20)-(22) with the boundary conditions (16) can be written:

$$Y_1'=Y_2,\quad Y_2'(1+3B\mathrm{W}^2{Y_2}^2)=A_1Y_1+A_2\tag{27}$$

$$Y_3'=Y_4,\quad Y_4'=-\mathrm{Ec}\,\mathrm{Pr}({Y_2}^2+B\mathrm{W}^2{Y_2}^4)-M\,\mathrm{Ec}\,\mathrm{Pr}(Y_1+1)^2-N_\mathrm{b}Y_4Y_6-N_\mathrm{t}Y_4^2+\gamma\,\mathrm{Pr}\,Y_3\tag{28}$$

$$Y_5'=Y_6,\quad Y_6'=S\,\mathrm{Sc}\,Y_5-\frac{N_\mathrm{t}}{N_\mathrm{b}}Y_4'\tag{29}$$

Subject to the boundary conditions:

$$\left.\begin{array}{l} Y_1=-1,\ Y_3=0 \text{ and } Y_5=0 \quad \text{at } h=-\eta \\ Y_1=1,\ Y_3=1 \text{ and } Y_5=1 \quad \text{at } h=\eta \end{array}\right\}\tag{30}$$

where the prime denotes to the differentiation with respect to y. To compute the physical quantities u, θ, and φ. MATHEMATICA package version 9 is used to solve the system of eqs. (27)-(29) with the boundary conditions (30).

The numerical solutions are compared with the perturbation solution through figs. 2-4.

Results and discussion

In the present section of the study, the effects of the physical parameters of the problem on the solutions obtained both analytically or numerically are discussed numerically and illustrated graphically through a set of figures. Also, a comparison between the analytical solutions and the numerical solutions are made. At the first figs. 2-4 clear that the results due to the analytical and numerical solutions obtained for velocity, temperature and nanoparticles are completely consistent and overlapped, and are convincing proof of the high accuracy of the perturbation method in solving non-linear differential equations compared to numerical method.

The graphs for velocity profile are described through figs. 5-9. Figures 10-15 demonstrate the variation of the temperature profile, the effects of various parameters on nanoparticle phenomena are discussed through figs. 16-19.

Velocity profile

The velocity, u, of the flow field is found to change more or less with the variation of the flow parameters. Figure 5 declares that the velocity increases with an increase in the value of the Hall parameter, m. This is due to the fact that an increase in m decreases the effective conductivity $\sigma/(1 + m^2)$, and hence the magnetic damping which clear in fig. 6. Figure 6 depicts the effect of the magnetic parameter, M, on the velocity distribution. Applications of magnetic field to an electrically conducting flow give rise to a resistive type of force called Lorenz force. This force has the tendency to slow down the motion of the fluid. As expected, as M increase the velocity decrease.

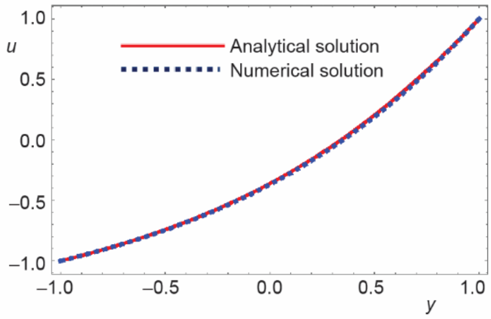

Figure 2. Comparison between analytical and numerical solutions of the velocity distribution, u, for different values of A = 0.2, M = 1.2, m = 1, p_0 = 0.5, n = 0.4, and W = 0.3

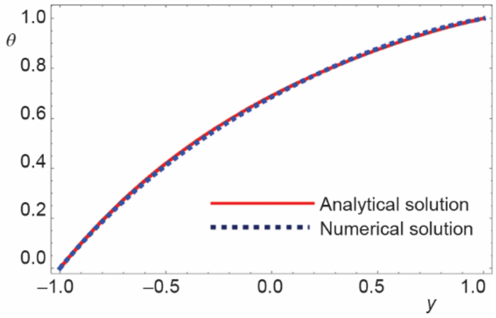

Figure 3. Comparison between analytical and numerical solutions of the temperature distribution θ for different values of A = 0.2, M = 1.2, m = 1, p_0 = 0.5, n = 0.4, W = 0.3, Pr = 0.7, Ec = 0.1, γ = 0.5, Sc = 0.15, S = 0.5, N_b = 1.5, and N_t = 0.5

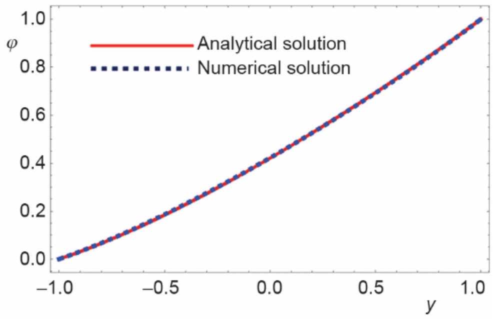

Figure 4. Comparison between analytical and numerical solutions of the nanoparticles phenomena, φ, for different values of A = 0.2, M = 1.2, m = 1, p_0 = 0.5, n = 0.4, W = 0.3, Pr = 0.7, Ec = 0.1, γ = 0.5, Sc = 0.15, S = 0.5, N_b = 1.5, and N_t = 0.5

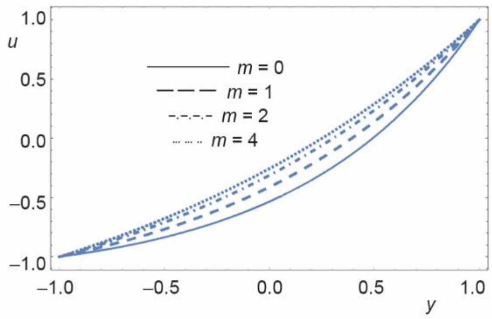

Figure 5. The velocity distribution, u, is plotted against y for different values of m when A = 0.2, M = 1.2, p_0 = 0.5, n = 0.4, and W = 0.3

Figure 7 depicts the behavior of the velocity under the effects of various values of Weissenberg number it is found that the velocity decreases with increasing Weissenberg number.

The influence of dimensionless power-law index, n, on velocity is illustrated in fig. 8, increasing n has a tendency to increase the velocity. Figure 9 illustrates the effect of the porosity parameter A on the velocity, it is clear that the velocity increases with increasing A.

Temperature profile

The variation of temperature profile for different values of the magnetic parameter, M, is plotted in fig. 10, it is clear that the temperature increases with increasing M.

The variation in the temperature distribution for different values of coefficient of heat absorption, γ, is given in fig. 11.

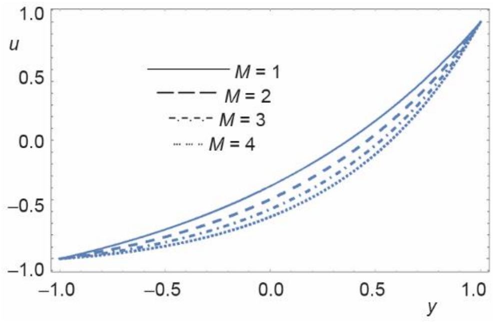

Figure 6. The velocity distribution, *u*, is plotted against *y* for different values of M when A = 0.2, m = 1, p_0 = 0.5, n = 0.4, and W = 0.3

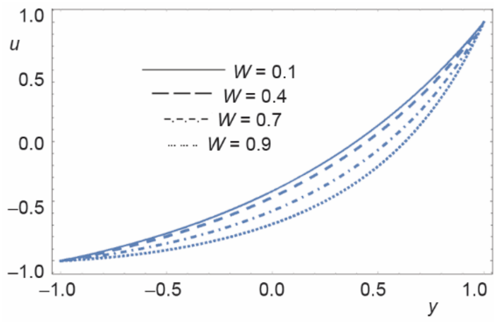

Figure 7. The velocity distribution, *u*, is plotted against *y* for different values of W when A = 0.2, m = 1, M = 1.2, n = 0.4, and p_0 = 0.5

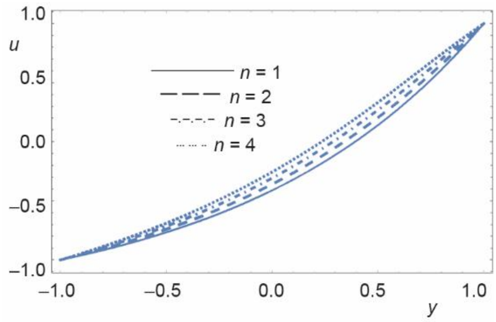

Figure 8. The velocity distribution, *u*, is plotted against *y* for different values of *n* when A = 0.2, m = 1, M = 1.2, W = 0.3, and p_0 = 0.5

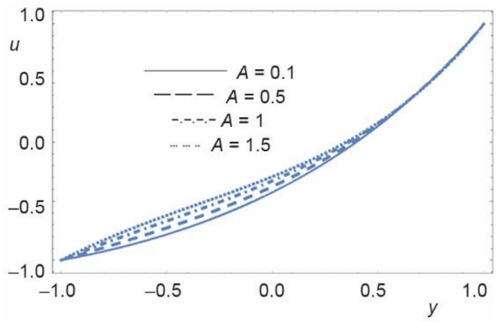

Figure 9. The velocity distribution, *u*, is plotted against *y* for different values of *A* when n = 0.4, m = 1, M = 1.2, W = 0.3, and p_0 = 0.5

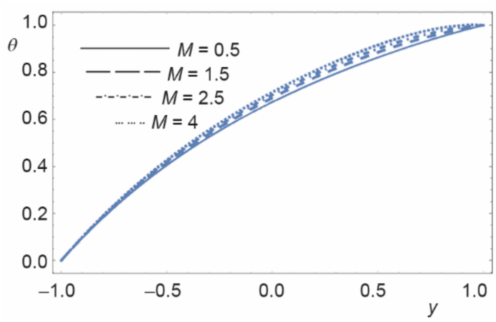

Figure 10. The temperature distribution, θ, is plotted against *y* for different values of *M* when A = 0.2, m = 1, p_0 0.5, n = 0.4, W = 0.3, Pr = 0.7,

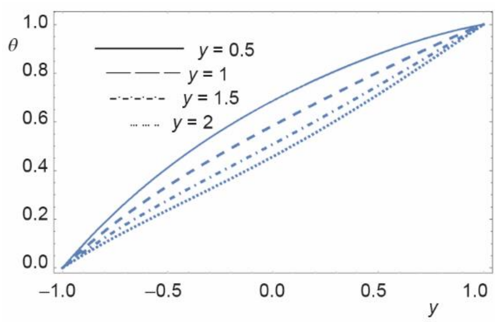

Figure 11. The temperature distribution, θ, is plotted against *y* for different values of γ when A = 0.2, m = 1, p_0 = 0.5, n = 0.4, W = 0.3, Pr = 0.7,

Ec = 0.1, γ = 0.5, Sc = 0.15, *S* = 0.5, N_b = 1.5, and N_t = 0.5

Ec = 0.1, *M* = 1.2, Sc = 0.15, *S* = 0.5, N_b = 1.5, and N_t = 0.5

It is noticed that an increase in the values of γ leads to decrease in the temperature. Figures 12 and 13 display the effects of the Brownian parameter, N_b, and the thermophoresis parameter, N_t, on the temperature distribution. There is a substantial increase in the temperature with an increase in N_b and N_t. As the Brownian motion and thermophoretic effects strengthen, this corresponds to the effective movement of nanoparticles from the wall to the fluid which results in the significant increase in the temperature.

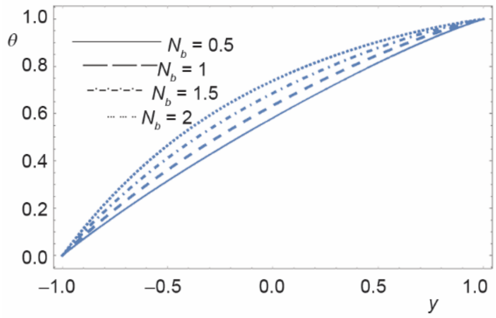

Figure 12. The temperature distribution, θ, is plotted against *y* for different values of N_b when *A* = 0.2, *m* = 1, p_0 = 0.5, *n* = 0.4, W = 0.3, Pr = 0.7, Ec = 0.1, γ = 0.5, Sc = 0.15, *S* = 0.5, *M* = 1.2, and N_t = 0.5

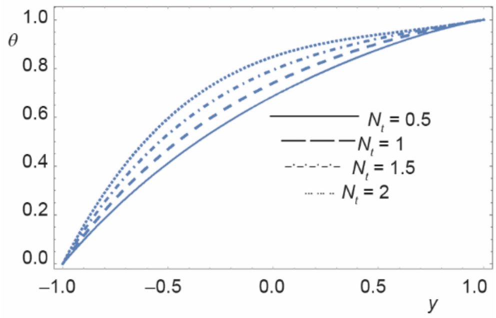

Figure 13. The temperature distribution, θ, is plotted against *y* for different values of N_t when *A* = 0.2, *m* = 1, p_0 = 0.5, *n* = 0.4, W = 0.3, Pr = 0.7, Ec = 0.1, γ = 0.5, Sc = 0.15, *S* = 0.5, *M* = 1.2, and N_b = 1.5

The temperature profile for different values of Prandtl number, and Eckert number are shown in figs. 14 and 15. It is distinguished that the temperature inside the fluid is forcefully diminished when Prandtl number is increased. Prandtl number is a proportion between momentum diffusivity and thermal diffusivity. At the point when the Prandtl number is increased, thermal diffusivity diminishes, which reduces the thermal layer thickness, while the temperature increases by increasing Eckert number.

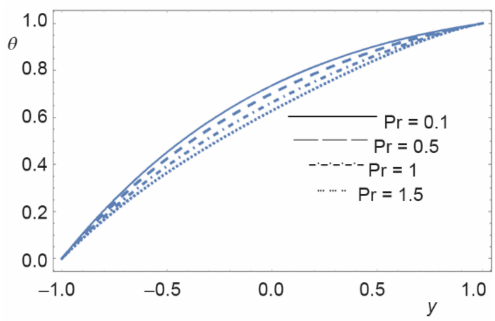

Figure 14. The temperature distribution, θ, is plotted against *y* for different values of Pr when *A* = 0.2, *m* = 1, p_0 = 0.5, *n* = 0.4, W = 0.3, N_b = 1.5,

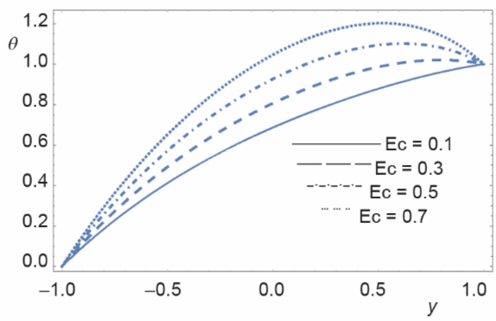

Figure 15. The temperature distribution, θ, is plotted against *y* for for different values of Ec when *A* = 0.2, *m* = 1, p_0 = 0.5, *n* = 0.4, W = 0.3,

Ec = 0.1, γ = 0.5, Sc = 0.15, S = 0.5, M = 1.2, and N_t = 0.5

N_b = 1.5, Pr = 0.7, γ = 0.5, Sc = 0.15, S = 0.5, M = 1.2, and N_t = 0.5

Nanoparticle phenomena

The nanoparticles phenomena distribution of the flow field is affected by four parameters, namely, the Schmidt number the chemical reaction coefficient, S, the Brownian parameter, N_b, and the thermophoresis parameter, N_t. Figures 16 and 17 illustrated the nanoparticles phenomena distribution for several values of the Schmidt number and the S. Schmidt number quantifies the relative effectiveness of momentum and mass transport by diffusion in hydrodynamic and nanoparticles. As the Schmidt number increase the nanoparticles phenomena decrease. The nanoparticles phenomena also decrease as the S increases.

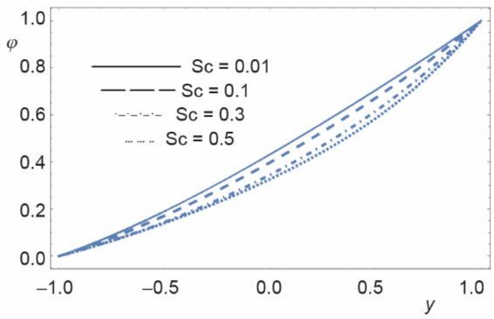

Figure 16. The nanoparticles phenomena, φ, is plotted against y for different values of Sc when A = 0.2, m = 1, p_0 = 0.5, n = 0.4, W = 0.3, N_b = 1.5, Pr = 0.7, γ = 0.5, Ec = 0.1, S = 0.5, M = 1.2, and N_t = 0.5

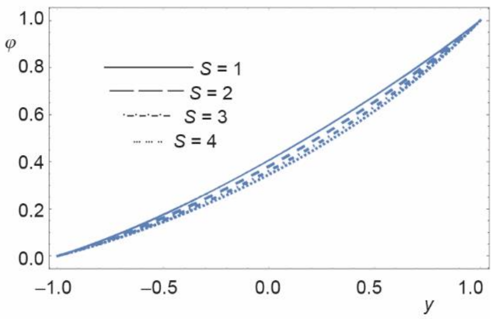

Figure 17. The nanoparticles phenomena, φ, is plotted against y for different values of S when A = 0.2, m = 1, p_0 = 0.5, n = 0.4, W = 0.3, N_b = 1.5, Pr = 0.7, γ = 0.5, Sc = 0.15, Ec = 0.1, M = 1.2, and N_t = 0.5

Figures 18 and 19 display the effects of the Brownian parameter, N_b, and the thermophoresis parameter, N_t, on the nanoparticles phenomena. There is a substantial increase in the nanoparticles phenomena with an increase in N_b. While the nanoparticles phenomena decrease by increasing the N_t.

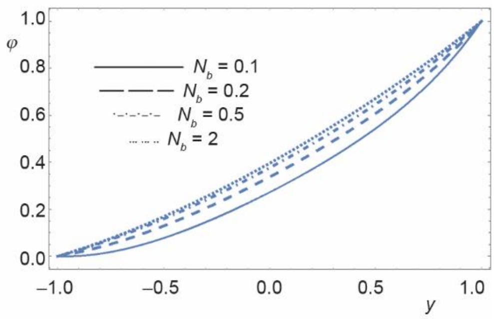

Figure 18. The nanoparticles phenomena, φ, is plotted against y for different values of N_b when A = 0.2, m = 1, p_0 = 0.5, n = 0.4, W = 0.3, S = 0.5,

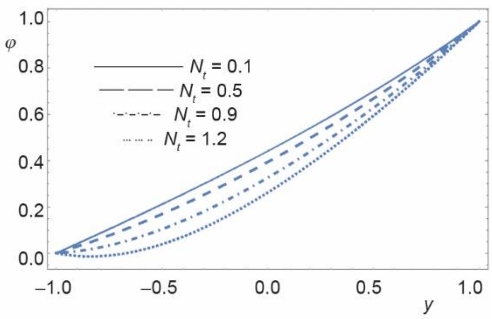

Figure 19. The nanoparticles phenomena, φ, is plotted against y for different values of of N_t when A = 0.2, m = 1, p_0 = 0.5, n = 0.4, W = 0.3,

Pr = 0.7, γ = 0.5, Sc = 0.15, Ec = 0.1, M = 1.2, and N_t = 0.5

S = 0.5, Pr = 0.7, γ = 0.5, Sc = 0.15, Ec = 0.1, M = 1.2, and N_b = 1.5

Conclusion

Analytical and numerical studies are made to obtain the solutions of the system of deferential equations which describe the peristaltic transport of a Carreau nanofluid through a porous medium in a symmetric horizontal channel. The effect of heat absorption, chemical reaction and Hall current with viscous dissipation are taken into account. The equations of motion are modulated and solved analytically by using perturbation technique and numerically by using Runge-Kutta-Merson method in a shooting and matching technique for velocity, temperature and nanoparticles phenomena. The effects of various emerging parameters are seen with the help of graphs. From the presented analysis some of the interesting observations are summarized as follows.

- The comparison between the analytical solutions and numerical solutions refers to the accuracy of analytical solutions compared to numerical solutions which appear in the matching curves.
- The velocity of the flow field increases by increasing the the Hall parameter, m, while it decreases by increasing values of the magnetic parameter, M.
- The effects of the Brownian parameter, N_b, and the thermophoresis parameter, N_t, on the temperature distribution increase the temperature.
- The temperature, θ, decrease with increasing the coefficient of heat absorption, γ, and Prandtl number.
- Increasing the magnitude of chemical reaction coefficient, S, led to decrease in the nanoparicles phenomena.
- The nanoparticles phenomena increase with an increase in N_b. While the nanoparticles phenomena decrease by increasing the N_t.

References

[1] Nadeem, S., *et al.*, Mathematical Model for the Peristaltic Flow of Nanofluid through Eccentric Tubes Comprising Porous Medium, *Appl. Nanosci., 4* (2014), 6, pp. 733-743
[2] Eldabe, N. T. M., *et al.*, Peristaltic Transport of Manetohydrodynamic Carreau Nanofluid with Heat and Mass Transfer inside Asymmetric Channel, *ACJM, 7* (2017), 1, pp. 1-20
[3] Palaniammal, S., Saritha, K., Heat and Mass Transfer of a Casson Nanofluid Flow over a Porous Surface with Dissipation, Radiation, and Chemical Reaction, *IEEE, 6* (2017), 6, pp. 909-918
[4] Prasad, K., *et al.*, Peristaltic Transport of a Nanofluid in an Inclined Tube, *American Journal of Computational and Applied Mathematics, 5* (2015), 4, pp. 117-128
[5] Mahbubul, I. M., *et al.*, Latest Developments on the Viscosity of Nanofluids, *International Journal of Heat and Mass Transfer, 55* (2012), 4, pp. 874-885
[6] Mustafa, M., *et al.*, Influence of Wall Properties on the Peristaltic Flow of a Nanofluid: Analytical and Numerical Solutions, *International Journal of Heat and Mass Transfer, 55* (2012), 17-18, pp. 4871-4877
[7] Ellahi, R., *et al.*, A Theoretical Study of Prandtl Nanofluid in a Rectangular Duct through Peristaltic Transport, *Appl. Nanosci., 4* (2014), 6, pp. 753-760
[8] Lakshminarayana, P., *et al.*, The Influence of Slip, Wall Properties on the Peristaltic Transport of a Conducting Bingham Fluid with Heat Transfer, *Procedia Engineering, 127* (2015), Dec., pp. 1087-1094
[9] Reddy, M. S., Raju, G. S. S., Non-Linear Peristaltic Pumping of Johnson-Segalman Fluid in an Asymmetric Channel under Effect of Magnetic Field, *European J. of Scientific Research, 46* (2010), 1, pp. 147-164
[10] Hayat, T., *et al.*, Heat Transfer Analysis for Peristaltic Mechanism in Variable Viscosity Fluid, *Chin. Phys. Lett., 4* (2011), 4, pp. 1-3
[11] Mahmoud, A. M, Abu Oda, N. A., Blood Flow in Uniform Planar Channel, *Asian J. of Applied Science 1* (2008), Jan., pp. 46-58

[12] Tanveer, A., *et al.*, Numerical Simulation for Peristalsis of Carreau-Yasuda Nanofluid in Curved Channel with Mixed Convection and Porous Space, *PloS One, 12* (2017), 2, ID e0170029
[13] Nowar, K., Peristaltic Flow of a Nanofluid under the Effect of Hall Current and Porous Medium, *Mathematical Problems in Engineering, 2014* (2014), ID 389581
[14] Kumar, P. M., *et al.*, Hall Effects on Peristaltic Flow of Couple Stress Fluid in a Vertical Asymmetric Channel, *Mathematical Science and Engineering, 263* (2017), 6, pp. 1-18
[15] Eldabe, N. T. M., *et al.*, Hall Effect on Peristaltic Flow of Third Order Fluid in a Porous Medium with Heat and Mass Transfer, *JAMP, 3,* (2015), 09, pp. 1138-1150
[16] Eldabe, N. T. M., *et al.*, Hall Effects on the Peristaltic Transport of Williamson Fluid through a Porous Medium with Heat and Mass Transfer, *Applied Mathematical Modelling, 40* (2016), 1, pp. 315-328

Paper submitted: March 19, 2019
Paper revised: June 26, 2019
Paper accepted: July 7, 2019